GAS-LIQUID FLOW AROUND AN OBSTACLE IN A VERTICAL PIPE - EXPERIMENT AND COMPUTATIONAL FLUID DYNAMICS SIMULATION

Horst-Michael Prasser, Thomas Frank[1], Mathias Beyer, Helmar Carl, Suleiman Al-Issa, Heiko Pietruske, and Peter Schütz

1. Introduction

In the frame of the TOPFLOW project, vertical pipe flow is experimentally studied in order to develop and validate models for bubble forces as well as for bubble coalescence and fragmentation in a gas-liquid two-phase flow. After a large number of experiments in plain vertical pipes [1, 2], which are the basis of the development for a multi-bubble size model for ANSYS CFX 10.0, the large test section with a nominal diameter of DN200 (Fig. 1) was used to study the flow field around an asymmetric obstacle (Fig. 2). This is an ideal test case for the Computational fluid dynamics (CFD) code validation, since the obstacle creates a pronounced three-dimensional two-phase flow field. Curved stream lines, which form significant angles with the gravity vector, a recirculation zone in the wake and a flow separation at the edge of the obstacle are phenomena widespread in real industrial components and installations, like bends, T-juctions, valves and safety valves. It has to be shown that the CFD-code predicts these phenomena well, after it has been equipped by new models, developed in simpler experimental geometries.

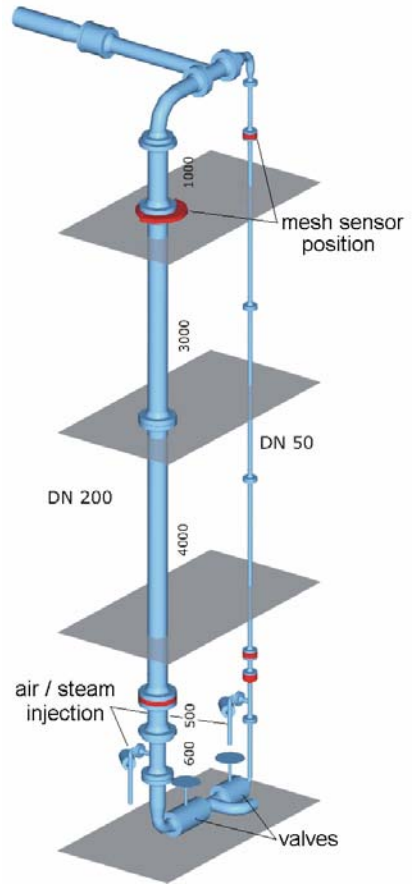

Fig. 1: Vertical test section DN200 of TOPFLOW

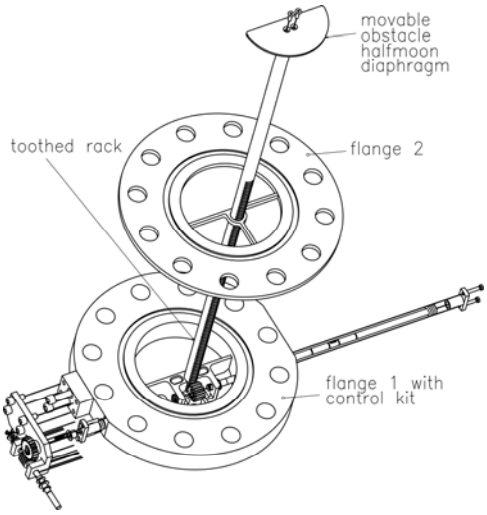

Fig. 2: Movable obstacle with drive support for TOPFLOW

Recently, test series were performed with an air-water flow at ambient conditions as well as with a steam-water mixture at a saturation pressure of 6.5 MPa [3]. Before the experiments were commissioned, an ANSYS CFX 10.0 pre-test calculation was carried out for one of the experimental tests.

[1] ANSYS Germany, Staudenfeldweg 12, 83624 Otterfing

2. Test arrangement

The test pipe has an inner diameter of 195.3 mm and a total height of 9 m. Water and gas are supplied from the bottom of the test section. The diaphragm (Fig. 2) is a half-moon shaped disk, the straight edge of which is arranged along the diameter of the pipe, while the circular edge is in a distance of 10 mm from the inner wall of the pipe. The disk is mounted on top of a toothed rod connected to a translation mechanism to change the axial position of the diaphragm.

Both obstacle and moving mechanism can be inverted and mounted either upstream or downstream of the wire-mesh sensor. The sensor was located 6.17 m downstream of the gas injection, when the obstacle was put upstream of the sensor. When the obstacle was put downstream of the sensor, the distance was 5.11 m. The arrangement allows to acquire local instantaneous void fractions from the full cross-section of the pipe with a spatial resolution of 3 mm and a rate of 2.5 kHz [4, 5] within the three-dimensional flow field around the diaphragm. The distance between sensor and diaphragm can be varied from 10 mm to a maximum distance of 520 mm without moving the sensor position, which is essential to perform high-pressure experiments in an efficient way, i.e. without dismantling and rearranging the test facility each time the measuring position has to be changed.

3. Test parameters

Measurements were carried out with an air-water flow at ambient pressure and a temperature of approximately 25 °C as well as with a steam-water mixture under saturation conditions at 6.5 MPa for the superficial velocities shown in Fig. 3. The following distances between diaphragm and mesh sensors were realized: $\Delta z = \pm 520$, ± 250, ± 160, ± 80, ± 40, ± 20, ± 15, ± 10 mm. Wire-mesh sensor signals were recorded after achieving a steady state for a measuring period of 10 s for each combination of boundary conditions. For each realized combination of superficial velocities data from both air and steam tests are available.

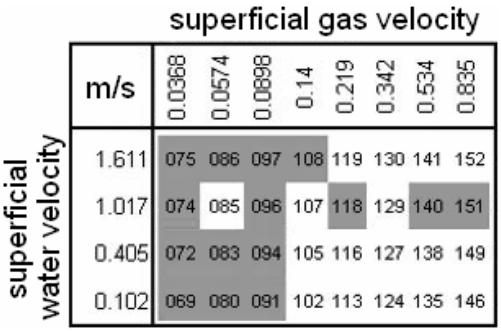

Fig. 3: Test matrix (grey: test points)

4. CFX pre-test calculations

Before the experiments were carry out a pre-test calculation was set-up for the boundary conditions of the air-water test 074 (see test matrix, Fig. 3), which was performed at the superficial velocities $J_L = 1.0$ m/s and $J_G = 0.037$ m/s. Flow conditions correspond to the bubbly flow regime. For the CFD simulation with ANSYS CFX 10.0 the Eulerian two-phase flow model was used [6, 7], assuming that the gaseous phase consists of monodisperse bubbles with a pipe elevation dependent equivalent diameter of 4.8-5.2 mm in order to account for the hydrostatic bubble expansion. Both phases were treated as non-compressible. Bubble drag in accordance to Grace drag law, Tomiyama lift force, Frank's generalized wall lubrication force and the turbulent dispersion force (with Favre Averaged Drag Model) have been taken into account [8]. Bubble coalescence and fragmentation were neglected for this first pre-test simulation, although it can be assumed that bubble fragmentation will take place at the edges of the obstacle and coalescence might become of importance in regions of bubble accumulation i.e. in the wake behind the obstacle.
Steady state simulations with ANSYS CFX 10.0 were performed on two numerical meshes created with ICEM CFD Hexa and consisting of about 119.000 and 473.000 hexahedral mesh ele-

ments. Meshes were generated for half of the TOPFLOW geometry assuming axial symmetry. The flow domain for the CFD simulation consisted of 1.5 m pipe sections up- and downstream of the obstacle. Inlet boundary conditions were set to fully developed two-phase pipe flow profiles for air and water velocities, radial gas volume fraction distribution, turbulent kinetic energy and turbulent eddy frequency. At the outlet cross section of the 3.0 m long pipe section an averaged static pressure outlet boundary condition was used.

5. Experimental results

5.1 Void fraction distribution

The sensor data was used to calculate two-dimensional time-averaged void fraction distributions in the measuring plane. By combining the information from measurements with different distances between sensor and diaphragm, full three-dimensional void distributions around the obstacle were obtained. A centre cut along the axis of the test pipe in a vertical plane perpendicular to the straight edge of the half-moon diaphragm is a very illustrative way to visualize the void fraction field. This was done in Fig. 4 for the field up- and downstream of the diaphragm.

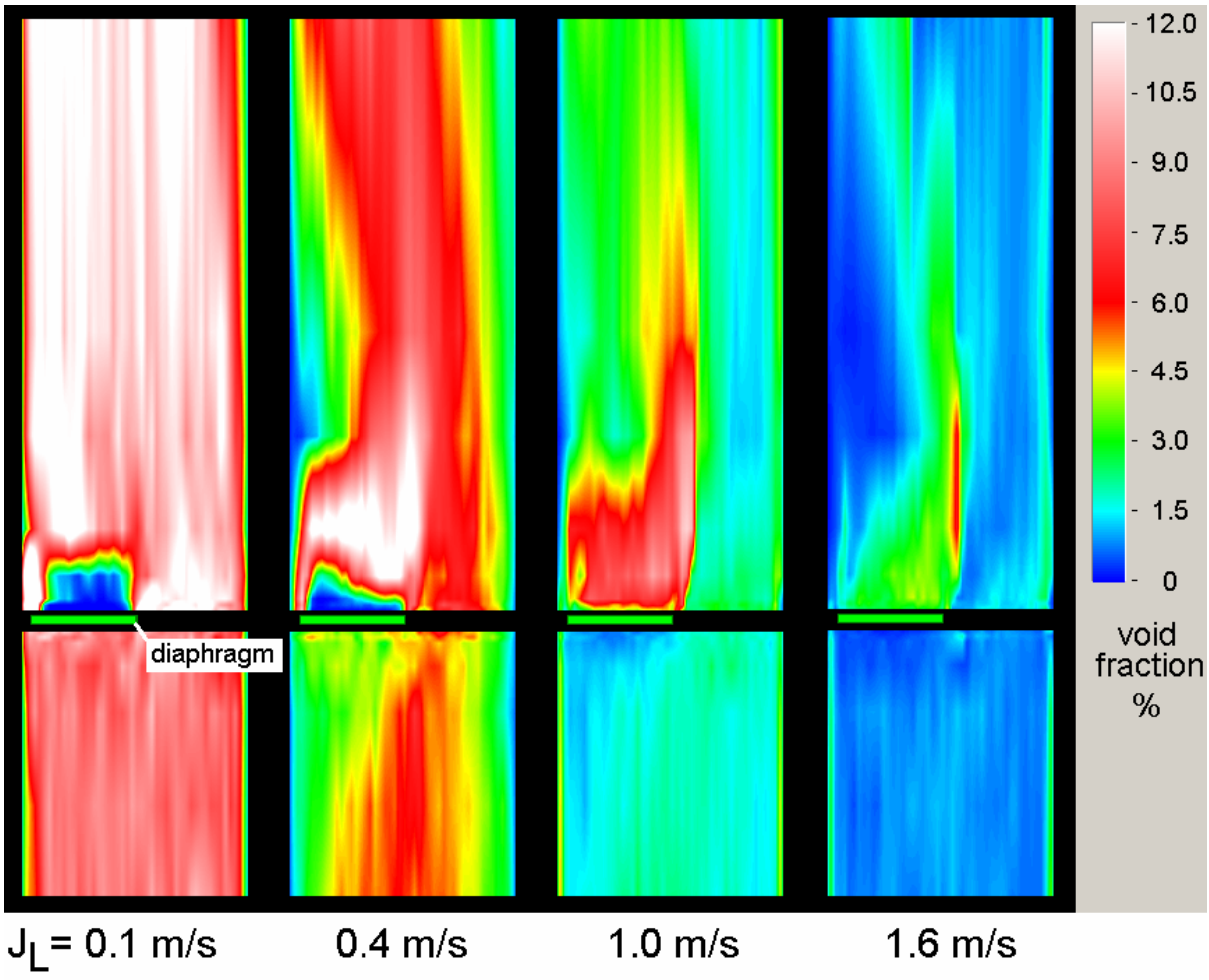

Fig. 4: Change of void fraction profiles up- and downstream of the diaphragm at J_G = 0.037 m/s with a variation of the superficial liquid velocity J_L

At small superficial water velocities, there is a region free of bubbles directly behind the obstacle, which vanishes with growing water velocity. The wake, i.e. the zone where a distortion of the

void field is found, grows in downstream direction with increasing liquid velocity, while the overall void fractions naturally decrease.

5.2 Horizontal bubble velocities

In the close vicinity of the eccentric diaphragm, bubbles were found to perform a sideward movement during their passage through the measuring plane of the sensor. This is caused by the bending of the streamlines. An estimation of the horizontal velocity component of the gaseous phase can be made by tracking the center of mass of the projection of each bubble onto the horizontal measuring plane during its passage. First, the coordinates of the centre of mass are calculated for each instant of the passage, followed by a linear regression of the coordinates as a function of time. The slope of the linear fit is interpreted as velocity components in x and y directions. An averaging of the velocity components is made in every measuring point of the sensor for all bubbles passing that point (normalized by void fraction).

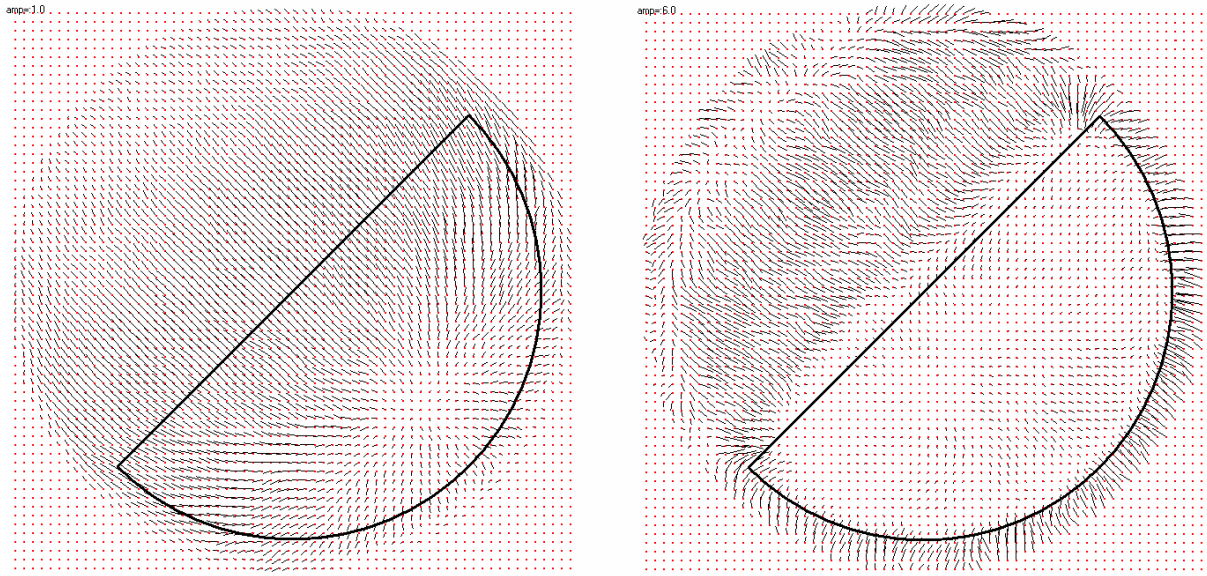

Fig. 5: Assessment of the horizontal velocity components by evaluation of the lateral movement of the center of mass of the bubble images during their passage through the sensor measuring plane, left: 40 mm upstream of the diaphragm, right: 40 mm downstream of the diaphragm, air-water test at J_L*=1 m/s and* J_G*=0.037 m/s*

As a result the two time-averaged velocity components v_x and v_y are obtained on the 64x64 measuring matrix. Vector plots are shown in Fig. 5 for both 40 mm upstream and, respectively, downstream of the diaphragm. These preliminary results show, that upstream of the diaphragm the velocity components in the x-y plane point away from the stagnation point. Downstream of the diaphragm, the tendency is inverted and vectors point back towards the recirculation zone that is found behind the diaphragm. This illustrates the large variety of information contained in the high-resolution mesh sensor data. The evaluation of the data will be continued.

5.3 Axial water velocities

There is a way to assess time-averaged local liquid velocities by evaluating the transit time of bubbles of a certain range of diameters. Due to the spatial resolution, the sensor data can be used to determine the lateral extension of each individual bubble by measuring the maximum area occupied by the bubble within the measuring plane during its passage [2, 5]. If a spherical bubble shape can be assumed, the diameter of a circle with an equivalent area divided by the time of the passage reveals the bubble velocity. A local instantaneous value of the liquid velocity is available after subtracting the bubble rise velocity. Time-averaged profiles of the axial liquid velocity are calculated by averaging individual values from a manifold of analysed bubbles.

Bubble deformation causes a systematic error that has to be eliminated by a calibration procedure. In order to keep the bubble deformation and the bubble rise velocity in a narrow band, velocities are calculated only from bubbles of a certain bubble size interval, which was set to 4-5 mm, so-called "marker bubbles". It was assumed that the bubble deformation can be accounted for by a calibration factor of the individual bubble velocity. This factor is determined by integrating the velocity profile found under the assumption of spherical bubbles over the cross-section and comparing the result with the known liquid superficial velocity.

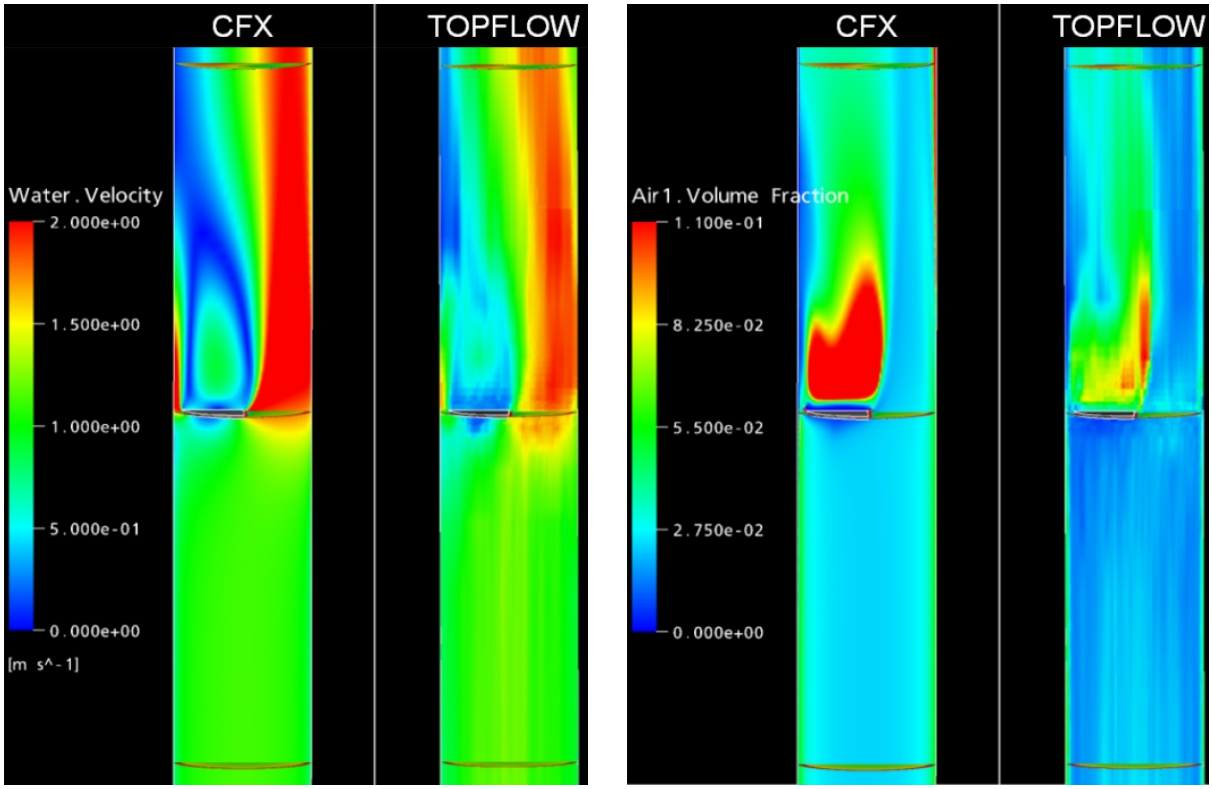

Fig. 6: Comparison between experiment and CFX pre-test calculation for the absolute water velocities (left) and the gas volume fraction distribution (right) for the region from 0.5 m upstream to 0.5 m downstream the obstacle; air-water test at J_L=1 m/s and J_G=0.037 m/s

The velocity distribution obtained in this way for the air-water test at J_L = 1 m/s and J_G = 0.037 m/s reports a recirculation zone behind the obstacle. It has to be kept in mind that the marker bubble method cannot supply information on the sign of the axial liquid velocity. Negative values expected in the centre of the recirculation zone can therefore not be reproduced and a local maximum is found instead (compare in Fig. 6, water velocities, the green zone above the obstacle).

By the estimation of liquid velocity profiles it becomes clear that the high gas fractions in the wake of the obstacle are caused by entrapping bubbles in the recirculation zone. Otherwise, upstream of the diaphragm the expected stagnation point is nicely reproduced and the concentration of the gaseous phase is decreased. Furthermore, the water velocity shows a maximum in the free cross-section area aside of the obstacle.

6. Comparison between the ANSYS CFX pre-test calculation and the experimental data

In preparation for the direct comparison of the CFD results and the experiments the 3-dimensional dataset from wire-mesh sensor measurements has been imported into the CFX graphical postprocessor. It makes it possible to use identical data processing and color schemes for visualization. Since experimental data have a fine (64×64) planar resolution in the x-y-plane but a limited coarser resolution in z-direction with respect to measuring planes, a pre-interpolation of the experimental data in z-direction has been applied with an axial resolution of the interpolated data with Δz=1mm.

Results for absolute water velocity and gas volume fraction distributions are shown in Fig. 6. The velocity field shows the same location and intensity both of the recirculation zone above and the stagnation regions under the obstacle surface. Smaller details, like the velocity and void fraction values above the gap between the circular edge of the obstacle and the inner wall of the pipe are also found in a good agreement. The reattachment length of the flow to the pipe wall downstream the obstacle is slightly increased in the CFD simulation, which is probably linked to the higher amount of entrained gas void fraction in the vortex behind the obstacle. Furthermore, the present simulation tends to overpredict the void fractions in the wake. This is a result of the assumption of a mono-disperse bubbly flow with a bubble size differing from reality and neglecting bubble coalescence with formation of larger bubbles in the wake of the obstacle. The agreement can be improved by using measured bubble-size distributions from the region upstream of the obstacle as a boundary condition for post-test calculations or by application of the inhomogeneous MUSIG model for the prediction of bubble size distributions from local flow conditions.

7. Conclusions

A novel technique to study the two-phase flow field around an asymmetric diaphragm in a vertical pipe is presented, that allows to produce data for CFD code validation in complex geometries. Main feature is a translocation of the diaphragm to scan the 3D void field with a stationary wire-mesh sensor. Besides time-averaged void fraction fields, a novel data evaluation method, was developed to extract estimated liquid velocity profiles from the wire-mesh sensor data. Furthermore, a new method for the estimation of horizontal velocity components of the gaseous phase is introduced.

A pre-test calculation done by ANSYS CFX 10.0 resulted in a good agreement with the experiment in terms of all significant qualitative details of the void fraction and velocity distributions. The structure and the geometry of the entire flow field in general as well as the dimensions of recirculation and stagnation zones in particular were predicted in good accordance with experimental data. The fact that for the time being a simple monodispers bubbly flow was assumed, led to an overestimation of void fractions especially in the wake of the obstacle, while the velocity profiles are matching better. It is planned to continue with post-test calculations in order to achieve a better quantitative agreement by using measured bubble-size distributions from the region upstream of the obstacle as inlet boundary condition and in a further step by applying the inhomogeneous MUSIG model for the prediction of bubble size distribution and bubble coales-

cence. The experimental data will be used to validate this recently developed and implemented model against detailed bubble size and bubble scale resolved void fraction measurements.

References

[1] Prasser, H.-M., Beyer, M., Böttger, A., Carl, H., Lucas, D., Schaffrath, A., Schütz, P., Weiss, F.-P., Zschau, J.: Influence of the pipe diameter on the structure of the gas-liquid interface in a vertical two-phase pipe flow, Nuclear Technology 152 (2005) 10. pp. 3-22.

[2] H.-M. Prasser, Influence of the Gas Injection on the Void Fraction Profiles and Bubble Size Distributions of a Air-Water Flow in Vertical Pipes, 5th ICMF'04, Yokohama, Japan, May 30–June 4, 2004, paper No.: 187.

[3] H.-M. Prasser, M. Beyer, H. Carl, H. Pietruske, P. Schütz: Steam-water experiments at high pressure to study the structure of the gas-liquid interface in a large vertical pipe, Annual Meeting on Nuclear Technology, Nuremberg, May 10-12, 2005, paper 215.

[4] H.-M. Prasser, D. Scholz, C. Zippe, 2001, Bubble size measurement using wire-mesh sensors, Flow Measurement and Instrumentation, 12/4, pp.299-312, 2001.

[5] H. Pietruske, H.-M. Prasser: Wire-mesh sensors for high-resolving two-phase flow studies at high pressures and temperatures, NURETH-11, Avignon, France, Oct. 2-6, 2005, paper No.: 533.

[6] ANSYS CFX 10.0 Users Manual, ANSYS Inc., July 2005.

[7] Th. Frank, J. Shi, A.D. Burns: "Validation of Eulerian multiphase flow models for nuclear reactor safety applications", 3rd TPFMI, Pisa, 22.-24. Sept. 2004, pp. 1-8.

[8] Th. Frank: Abschlussbericht zum Forschungsvorhaben 150 1271 "Entwicklung von CFD-Software zur Simulation mehrdimensionaler Strömungen im Reaktor-kühlsystem", ANSYS Germany, Technical Report TR-06-01, Januar 2006, pp. 1-72.

Acknowledgements

The work is carried out as a part of current research projects funded by the German Federal Ministry of Economics and Labour, project numbers 150 1265 and 150 1271. Electronic equipment for wire-mesh sensors was developed in co-operation with TELETRONIC GmbH (www.tz-rotech.de/teletronic/). The authors express their gratitude to the technical TOPFLOW team.